Brain Struct Funct
DOI 10.1007/s00429-013-0643-2

ORIGINAL ARTICLE

Exclusive neuronal expression of SUCLA2 in the human brain

Arpád Dobolyi · Elsebet Ostergaard · Attila G. Bagó · Tamás Dóczi · Miklós Palkovits · Aniko Gál · Mária J. Molnár · Vera Adam-Vizi · Christos Chinopoulos

Received: 8 July 2013 / Accepted: 18 September 2013

Abstract *SUCLA2* encodes the ATP-forming β subunit (A-SUCL-β) of succinyl-CoA ligase, an enzyme of the citric acid cycle. Mutations in *SUCLA2* lead to a mitochondrial disorder manifesting as encephalomyopathy with dystonia, deafness and lesions in the basal ganglia. Despite the distinct brain pathology associated with *SUCLA2* mutations, the precise localization of SUCLA2 protein has never been investigated. Here, we show that immunoreactivity of A-SUCL-β in surgical human cortical tissue samples was present exclusively in neurons, identified by their morphology and visualized by double labeling with a fluorescent Nissl dye. A-SUCL-β immunoreactivity co-localized >99 % with that of the d subunit of the mitochondrial F_0–F_1 ATP synthase. Specificity of the anti-A-SUCL-β antiserum was verified by the absence of labeling in fibroblasts from a patient with a complete deletion of *SUCLA2*. A-SUCL-β immunoreactivity was absent in glial cells, identified by antibodies directed against the glial markers GFAP and S100. Furthermore, in situ hybridization histochemistry demonstrated that *SUCLA2* mRNA was present in Nissl-labeled neurons but not glial cells labeled with S100. Immunoreactivity of the GTP-forming β subunit (G-SUCL-β) encoded by *SUCLG2*, or in situ hybridization histochemistry for *SUCLG2* mRNA could not be demonstrated in either neurons or astrocytes. Western blotting of post mortem brain samples revealed minor G-SUCL-β immunoreactivity that was, however, not upregulated in samples obtained from diabetic versus non-diabetic patients, as has been described for murine brain. Our work establishes that SUCLA2 is expressed exclusively in neurons in the human cerebral cortex.

Keywords Succinate thiokinase · Succinyl coenzyme A synthetase · Substrate-level phosphorylation · mtDNA · Neuronal mitochondrial marker

Introduction

Succinyl-CoA ligase [(SUCL), also known as succinyl coenzyme A synthetase (SCS), or succinate thiokinase

Electronic supplementary material The online version of this article (doi:10.1007/s00429-013-0643-2) contains supplementary material, which is available to authorized users.

A. Dobolyi · A. G. Bagó · M. Palkovits
Department of Anatomy, Histology and Embryology, Semmelweis University, Budapest 1094, Hungary

E. Ostergaard
Department of Clinical Genetics, Copenhagen University Hospital Rigshospitalet, 2100 Copenhagen, Denmark

A. G. Bagó
National Institute of Neurosurgery, Budapest 1145, Hungary

T. Dóczi
MTA-PTE Clinical MR Research Group, Department of Neurosurgery, University of Pécs, Pecs 7623, Hungary

M. Palkovits
Human Brain Tissue Bank, Semmelweis University, Budapest 1094, Hungary

A. Gál · M. J. Molnár
Institute of Genomic Medicine and Rare Disorders, Semmelweis University, Budapest 1083, Hungary

V. Adam-Vizi · C. Chinopoulos (✉)
Department of Medical Biochemistry, Semmelweis University, Hungarian Academy of Sciences, SE Laboratory for Neurobiochemistry, Budapest 1094, Hungary
e-mail: chinopoulos.christos@eok.sote.hu

Published online: 02 October 2013

(STK)] is a heterodimeric enzyme, composed of an invariant α subunit encoded by *SUCLG1* and a substrate-specific β subunit, encoded by either *SUCLA2* or *SUCLG2*. This dimer combination results in either an ATP-forming (EC 6.2.1.5) or a GTP-forming SUCL (EC 6.2.1.4). The enzyme is located in the mitochondrial matrix being part of the citric acid cycle, catalyzing the conversion of succinyl-CoA and ADP (or GDP) to CoASH, succinate and ATP (or GTP) (Johnson et al. 1998). ΔG for this reaction is 0.07 kJ/mol and therefore it is reversible (Li et al. 2013). When SUCL proceeds in the direction towards succinyl-CoA, this product may follow heme- or ketone body metabolism (Labbe et al. 1965; Ottaway et al. 1981). On the other hand, the reaction proceeding towards ATP or GTP formation is termed 'substrate-level phosphorylation' and can occur in the absence of oxygen. Substrate-level phosphorylation during anoxia/ischemia rescues cells from cytosolic ATP depletion (Chinopoulos et al. 2010, 2013; Kiss et al. 2013). GTP is a central regulator of cellular anabolism (Pall 1985); in mitochondria, GTP is used by the protein synthesis machinery, the PEP carboxykinase isoform 2 and GTP-AMP phosphotransferase and other GTP-binding proteins (Thomson 1998). GTP salvage inside the matrix is critical because it is believed not to be transported through the inner mitochondrial membrane in higher organisms (Pfaff et al. 1965). However, guanine nucleotide transport by atractyloside-sensitive and -insensitive mechanisms in isolated heart mitochondria has been reported by one group (McKee et al. 1999, 2000), but the carrier has not been found. On the other hand, it is well established that yeasts harbor a mitochondrial GTP/GDP translocase, but a homologue in higher organisms has not been identified (Vozza et al. 2004); accordingly, yeasts lack a GTP-forming SUCL (Przybyla-Zawislak et al. 1998). GTP-forming SUCL may support ATP formation in the matrix through the concerted action with a mitochondrial isoform of a nucleotide diphosphate kinase known as nm23-H4; this kinase complexes with either ATP- or GTP-forming SUCL (Kadrmas et al. 1991; Kowluru et al. 2002).

Considering the extensive involvement of SUCL in vital biochemical pathways, it is not surprising that its deficiency leads to serious pathology. The disease phenotype matches the tissue-specific expression of its subunits: A-SUCL-β is highly expressed in skeletal muscle, brain and heart, while G-SUCL-β is barely detected in brain and muscle, but strongly expressed in liver and kidney (Lambeth et al. 2004). Accordingly, mutations in *SUCLA2* (MIM ID #612073) results in Leigh's or a Leigh-like syndrome with onset of severe hypotonia in early childhood, muscular atrophy and sensorineural hearing impairment often leading to death during childhood. Neuroimaging findings include basal ganglia involvement, especially affecting the putamen and the caudate nuclei (Carrozzo et al. 2007), demyelination and atrophy (Ostergaard et al. 2007b). *SUCLA2* deficient patients show no abnormalities related to liver functions. Mutations in the α subunit-encoding *SUCLG1* gene have been reported in 16 patients (Ostergaard et al. 2007a, 2010) and they are associated with a phenotype similar to that seen in patients with *SUCLA2* deficiency, or a fatal infantile lactic acidosis. Mutations in the *SUCLG2* gene have not been reported so far, and may be incompatible with life.

SUCL deficiency is associated with mtDNA depletion, characterized by a massive reduction of mitochondrial DNA content. Three main clinical presentations of mtDNA depletion syndrome (MDS) are known: (a) myopathic, (b) encephalomyopathic and (c) hepatocerebral, depending on the tissues affected and their residual mitochondrial DNA levels (Rotig and Poulton 2009). *SUCLA2* deficiency is associated with the encephalomyopathic tier. mtDNA depletion (15–40 % residual amount) was found in the muscle samples of such patients (Ostergaard 2008). However, mtDNA depletion was found in fibroblasts from patients with *SUCLA2* deficiencies of only two out of four patients in one study (Carrozzo et al. 2007), while in (Miller et al. 2011) mtDNA depletion was evident only after serum deprivation which could be ameliorated by supplementation of deoxyribonucleosides. Data on brain biopsies from *SUCLA2* deficiency patients are not available. In the most comprehensive study in terms of extensive biopsies from patients with MDS, samples were collected from muscle, liver, blood or fibroblasts, but not brain (Navarro-Sastre et al. 2012). Yet, in *SUCLA2* deficiency it is the brain that seems to be the most vulnerable tissue, as *SUCLG2* and *nm23-H4* are only weakly expressed (Milon et al. 1997; Lambeth et al. 2004). SUCL forms a physical complex with nm23-H4, the lack of which hinders the kinase function leading to a defect in the last step of the mitochondrial nucleotide salvage pathway (Elpeleg et al. 2005), thus causing mtDNA depletion (Ostergaard et al. 2007a, 2010)

Fibroblasts and skeletal muscle are homogeneous tissues (despite the different categories of muscle fiber types); however, the brain consists of several different cell types, the major categories being neurons and glial cells. There is an obvious gap of knowledge regarding the pathophysiology of *SUCLA2* deficiency in the brain, the organ that suffers the most from this inborn error of metabolism. Analysis of expression of SUCLA2 in the human brain has been reported only once, but in that report cell- or region-specific expression was not investigated (Lambeth et al. 2004). In this study, we show unequivocally that SUCLA2 is expressed exclusively in the neurons of the human brain.

Results

The specificity of SUCLA2 and SUCLG2 immunoreactivity in human tissues

The specificity of SUCLA2 immunoreactivity was validated using human fibroblasts from a control subject versus those from a patient suffering from a complete deletion in *SUCLA2* gene. The specificity of SUCLG2 immunoreactivity was validated using HEK293 cells, see Fig. 1. The mitochondrial network was selectively stained by loading cells with Mitotracker Orange (MTO, 1 μM, red) prior to fixation, see panels A2 (control fibroblasts), B2 (SUCLA2-deficient fibroblasts) and C2 (HEK293 cells). Normal human fibroblasts were strongly labeled with the procedure of SUCLA2 immunostaining (panel A1, green), and there was a robust co-localization with the decoration obtained by MTO (panel A3, yellow). In contrast, fibroblasts derived from the patient lacking *SUCLA2* did not show SUCLA2 immunolabeling (panel B1), while the mitochondrial network outlined by MTO was unremarkable (panel B2, red), and accordingly there was no SUCLA2 immunoreactivity-MTO co-localization (panel B3). For validating the antibody raised against SUCLG2 we immunolabeled HEK293 cells which exhibit a very high expression of this protein (Tanner et al. 2007); confocal images of G-SUCL-β immunolabeling in these cells are shown in panel C1 (green). MTO labeling was intense (panel C2, red), and the extent of co-localization was also evident, shown in panel C3 (yellow). The scale bar is 20 μm.

SUCLA2 immunoreactivity and absence of SUCLG2 immunoreactivity in the human frontal and temporal cortical samples

SUCLA2 antibody labeled a large number of cells in both the frontal and temporal cortex with no visible difference between the male and female human brain (Fig. 2a). The labeled cells were numerous in all layers of the cortices except layer I. The labeled cells demonstrated different morphologies. A number of large pyramidal cells were labeled but smaller cells also showed SUCLA2 immunoreactivity. In general, SUCLA2 immunoreactivity was present within the cell bodies as well as the proximal dendrites but not in the nuclei (Fig. 2a, b). The same procedure but for SUCLG2 immunoreactivity applied for HEK293 cells or using more concentrated or more diluted antiserum resulted in no specific cellular labeling in the human frontal and temporal cortical samples (Fig. 2c), in accordance with the original report by the group of Lambeth (Lambeth et al. 2004). It is to be noted that *SUCLG2* for humans exhibits transcript variants. However, all transcripts are identical in the region 1–396, except in position 220 (see supplemental Fig. 1). The antibody that we used to identify SUCLG2 (Abcam, Cat. No. #ab96172) was raised by immunizing rabbits with a recombinant fragment corresponding to a region within the N terminal amino acids 1–204 of human SUCLG2. Therefore, it should not be able to distinguish among transcript variants.

The mitochondrial localization of SUCLA2 immunoreactivity

The labeling of SUCLA2 within the neurons is punctate with a cellular localization resembling that of mitochondria, suggesting the presence of SUCLA2 immunoreactivity in this organelle (Fig. 3a1, b1). Although in situ mitochondria are normally filamentous, cellular stress as it may be the case during handling of the specimen or simply postmortem delay will cause mitochondrial fragmentation, yielding a punctate appearance. To identify the mitochondrial presence of SUCLA2, co-localization studies were performed for F_0–F_1 ATP synthase subunit d. The distribution of F_0–F_1 ATP synthase subunit d delineated the expected distribution of mitochondria (Fig. 3a2, b2). Furthermore, an almost complete co-localization of SUCLA2 and F_0–F_1 ATP synthase subunit d and the absence of singly labeled structures indicate the exclusively mitochondrial localization of SUCLA2 (Fig. 3a3, b3).

Identification of cell types containing SUCLA2 immunoreactivity in the human temporal cortex

The distribution of SUCLA2-immunoreactive cells is similar to that of neurons: they are present in all layers of the temporal cortex but their density is small in layer I (Fig. 4a1, b1). SUCLA2 immunoreactivity was present in 88 % of cells identified as neuron based on its larger, less irregular shape in Nissl staining (Fig. 4a2). In contrast, dark Nissl-labeled cells, possibly glial cells do not contain SUCLA2 at all (Fig. 4a2). Unfortunately, labeling with NeuN (clone BBS/NC/VI-H14) or neuron-specific enolase used for the immunocytochemical identification of neurons did not label our human brain sections consistently to confirm the neuronal location of SUCLA2 immunoreactivity. Instead, we used glial markers to confirm the absence of SUCLA2 immunoreactivity in these cell types. Indeed, a lack of co-localization of SUCLA2 and S100, an astrocyte marker suggested that SUCLA2 was absent in astrocytes (Fig. 4b1, b2, b3). In addition, the glial marker GFAP also showed a different distribution from SUCLA2 immunoreactive cells and did not co-localize with SUCLA2 immunoreactivity (Fig. 5).

The presence of SUCLA2 but not SUCLG2 mRNA in the human temporal cortex

A single band appeared on gels following RT-PCR using all primer pairs specific to *SUCLA2* and *SUCLG2* when cDNA

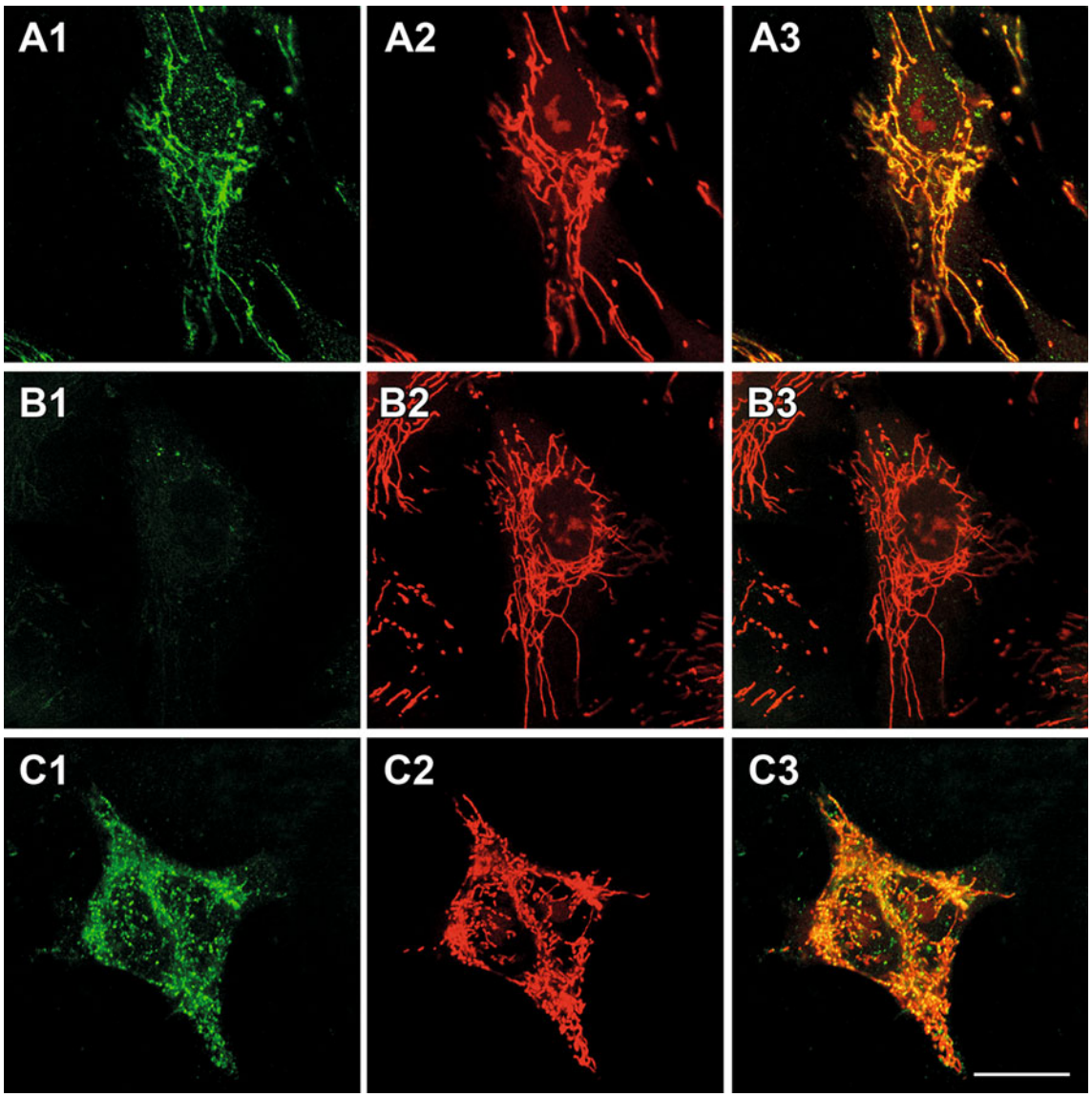

Fig. 1 Co-immunolabeling of human fibroblasts (SUCLA2) and HEK293 cells (SUCLG2) with Mitotracker Orange (MTO). **a1** SUCLA2 immunoreactivity in normal human fibroblasts. Intracellular structures resembling mitochondria are intensely labeled. **a2** MTO labeling outlining the mitochondrial network in normal human fibroblasts. **a3** Merged image of SUCLA2 immunodecoration with MTO labeling. **b1** Specific labeling for SUCLA2 is absent in fibroblasts derived from the patient lacking SUCLA2. **b2** MTO staining outlining the mitochondrial network in the fibroblasts obtained from the patient lacking SUCLA2. **b3** Merged image of SUCLA2 immunodecoration with MTO labeling, revealing lack of co-localization. **c1** SUCLG2 labels HEK293 cells. **c2** MTO labeling outlining the mitochondrial network in HEK293 cells. **c3** Merged image of SUCLG2 immunodecoration with MTO labeling in HEK293 cells. *Scale bar* 20 μm

from human fibroblasts were used (Fig. 6a). However, when human temporal cortical cDNA was used, the same molecular weight products appeared only with *SUCLA2* primers albeit with a smaller bandwidth. In contrast, *SUCLG2* primers produced extremely faint bands. It must be noted that a cDNA clone containing a complete ORF for *SUCLG2* obtained from the human hippocampus appears in the literature (Strausberg et al. 2002). In our RT-PCR experiments very weak signals may well originate from *SUCLG2* mRNA of lymphocytes, endothelial cells or pericytes of vessels present in the specimen. The lengths of the PCR products were consistent with the lengths calculated from the position of the corresponding primer pair (Fig. 6a). PCR reactions without cDNA template were always included, and we did not detect bands in these negative controls (not shown).

The distribution of mRNA expression of SUCLA2 in the human temporal cortex

In situ hybridization histochemistry revealed the distribution of mRNA of *SUCLA2* (Fig. 6b), whereas that of SUCLG2 was not detected in the human temporal cortex

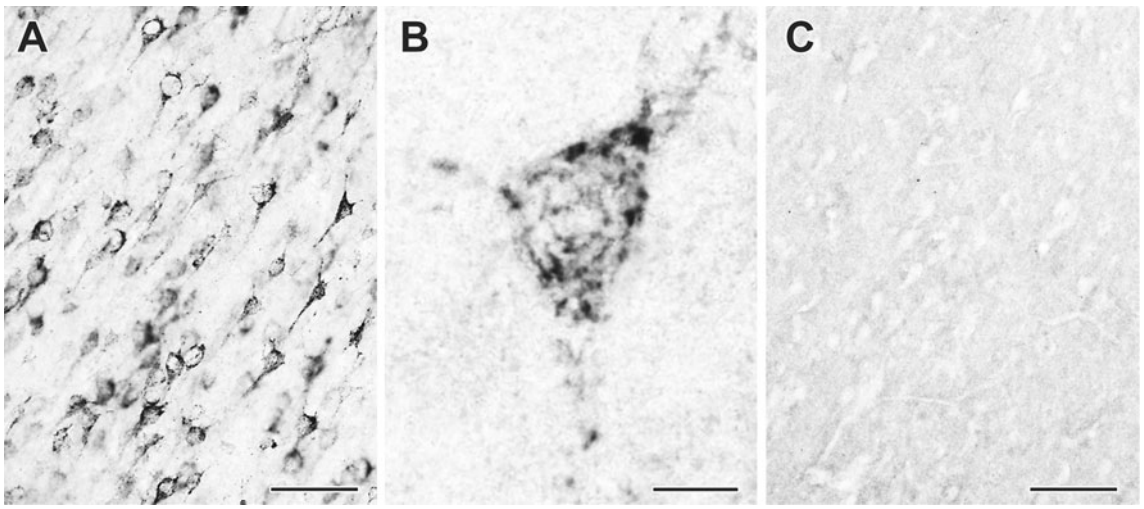

Fig. 2 Immunolabeling for SUCLA2 but not SUCLG2 in the human temporal cortex. **a** SUCLA2-immunoreactive cells with DAB visualization are evenly distributed in layer V of the human temporal cortex. **b** A large magnification picture demonstrates distribution of SUCLA2 immunoreactivity that resembles to that of mitochondria within a labeled cell. **c** SUCLG2 immunoreactivity is absent in the human temporal cortex. *Scale bar*s 50 μm for **a** and **c**, and 10 μm for **b**

(Fig. 6c), in agreement with the immunohistochemistry and RT-PCR results shown above, and the earlier results by the group of Lambeth (Lambeth et al. 2004). This result also verifies that the absence of G-SUCL-β immunoreactivity is genuine, and does not reflect a technical limitation of the antibody in our immunohistochemistry and/or Western blotting protocols. The two antisense probes for *SUCLA2* resulted in identical hybridization patterns; therefore, they will not be separately described. In the temporal cortex, all layers contained *SUCLA2* mRNA, whereas the corpus callosum (cc) did not show any labeling. The intensity of labeling was the highest in the pyramidal layers containing large pyramidal cells (Fig. 6b). The intensity of labeling was lower in layer VI and in the superficial layers. In particular, layer I contained only a small number of cells expressing *SUCLA2*. In the human temporal cortical brain sections labeled for SUCLA2 mRNA, Nissl-labeled cells as well as S100-immunoreactive cells were present. The distribution of Nissl-labeled neurons (Fig. 7a) was similar to that of SUCLA2-expressing cells, whereas S100-immunoreactive glial cells had a more even distribution pattern (Fig. 7b). Furthermore, high-magnification pictures indicated that over 90 % of Nissl-labeled neurons exhibited *SUCLA2* mRNA (Fig. 7c) while 95 % of *SUCLA2* mRNA-expressing cells were identified as neurons based on Nissl labeling in the human temporal cortex. In contrast, the distribution of SUCLA2 mRNA-expressing cells was different from that of S100-immunoreactive cells in high-magnification pictures (Fig. 7d) and *SUCLA2* mRNA-expressing cells showed less than 5 % co-localization with S100 immunoreactivity.

SUCLA2 and SUCLG2 immunoreactivities in homogenates from various brain regions

The antibody directed against SUCLA2 worked in immunohistochemistry protocols only from fresh human brain specimens. However, the antibody recognized reliably SUCLA2 in samples that have been preserved in our Brain Tissue Bank for prolonged periods of time which were processed for Western blotting. This provided the opportunity to examine the presence of SUCLA2 from several brain regions. As shown in Fig. 8 panel A, homogenate samples obtained from three different donors (Table 1a, b) from temporal cortex, caudate nucleus, putamen, frontal cortex, white matter and cerebellar cortex tested positive for SUCLA2 immunoreactivity. Even though white matter does not contain neuronal cell bodies it still exhibited significant SUCLA2 immunoreactivity, probably originating from the mitochondria found along the axons. 'MB' signifies mouse brain homogenates from four different animals (numbered as 1, 2, 3 and 4). In this and the other panels of Fig. 8, β-actin immunoreactivity served as a loading control for all lanes.

The specificity of the SUCLA2 antibody is certified by the blot shown in panel B, where there was no immunoreactivity from fibroblasts of a patient suffering from complete deletion of the *SUCLA2* gene.

SUCLG2 immunoreactivity (panel A) was extremely weak in the human brain samples, as compared to the mouse brain samples, in accordance with the results of previous Western blot experiments (Kiss et al. 2013). As for the case of RT-PCR results, such weak SUCLG2

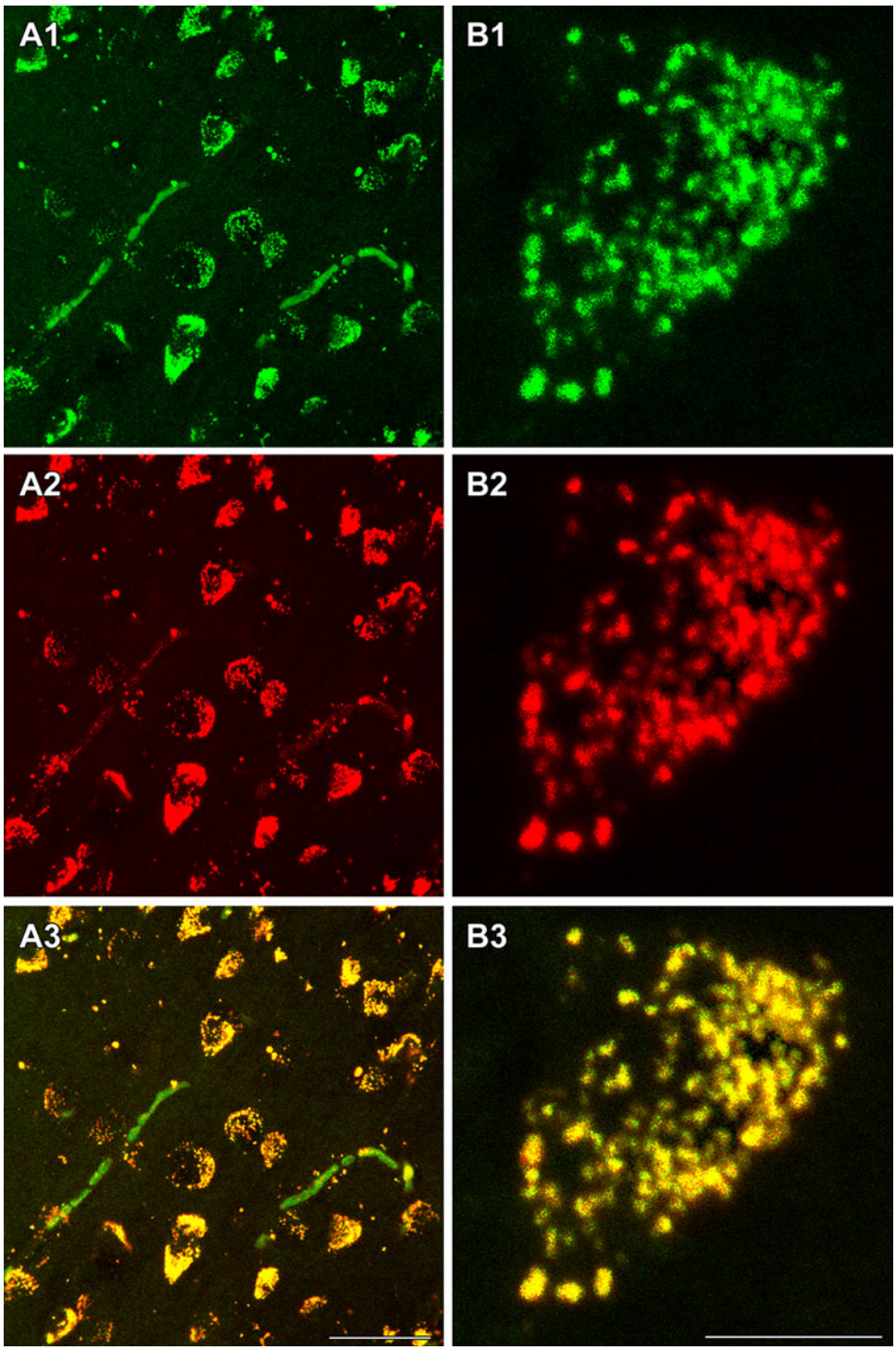

Fig. 3 The mitochondrial localization of SUCLA2 based on its co-localization with the d subunit of the F_0–F_1 ATP synthase. **a1** SUCLA2 immunoreactivity in the human temporal cortex visualized by FITC-tyramide amplification immunofluorescence. Red blood cells in some capillaries are labeled because of their endogenous peroxidase activity. **b1** A high-magnification confocal image demonstrates the localization of SUCLA2 within a SUCLA2-positive cell. **a2** Distribution of the immunoreactivity of the mitochondrial marker F_0–F_1 ATP synthase subunit d in the same field as **a1**. **b2** F_0–F_1 ATP synthase subunit d immunoreactivity in the same field as B1. **a3** *Yellow color* indicates co-localization of SUCLA2 and F_0–F_1 ATP synthase subunit d. An almost complete absence of singly labeled structures can be observed except for the red blood cells. **b3** The co-localization of SUCLA2 and F_0–F_1 ATP synthase subunit d is predominant even within a cell at high magnification. *Scale bars* 50 μm for **a1**–**a3** and 20 μm for **b1**–**b3**

immunoreactivity in human brain homogenates may originate from trapped lymphocytes, endothelial cells or pericytes from vessels present in the specimen, and not being genuine to neurons or glial cells. Although there are no tissues available with null expression of SUCLG2 (as in the case for the fibroblasts from the patient suffering from complete deletion of the SUCLA2 gene), the fact that the bands obtained from mouse tissues and the human specimens appeared at the exact same molecular weight affords a reasonable degree of assurance that SUCLG2 immunoreactivity is indeed genuine.

In the rat brain, streptozotocin-induced diabetes upregulates GTP-forming succinyl-CoA ligase activity more than ten times (Jenkins and Weitzman 1986). Mindful of

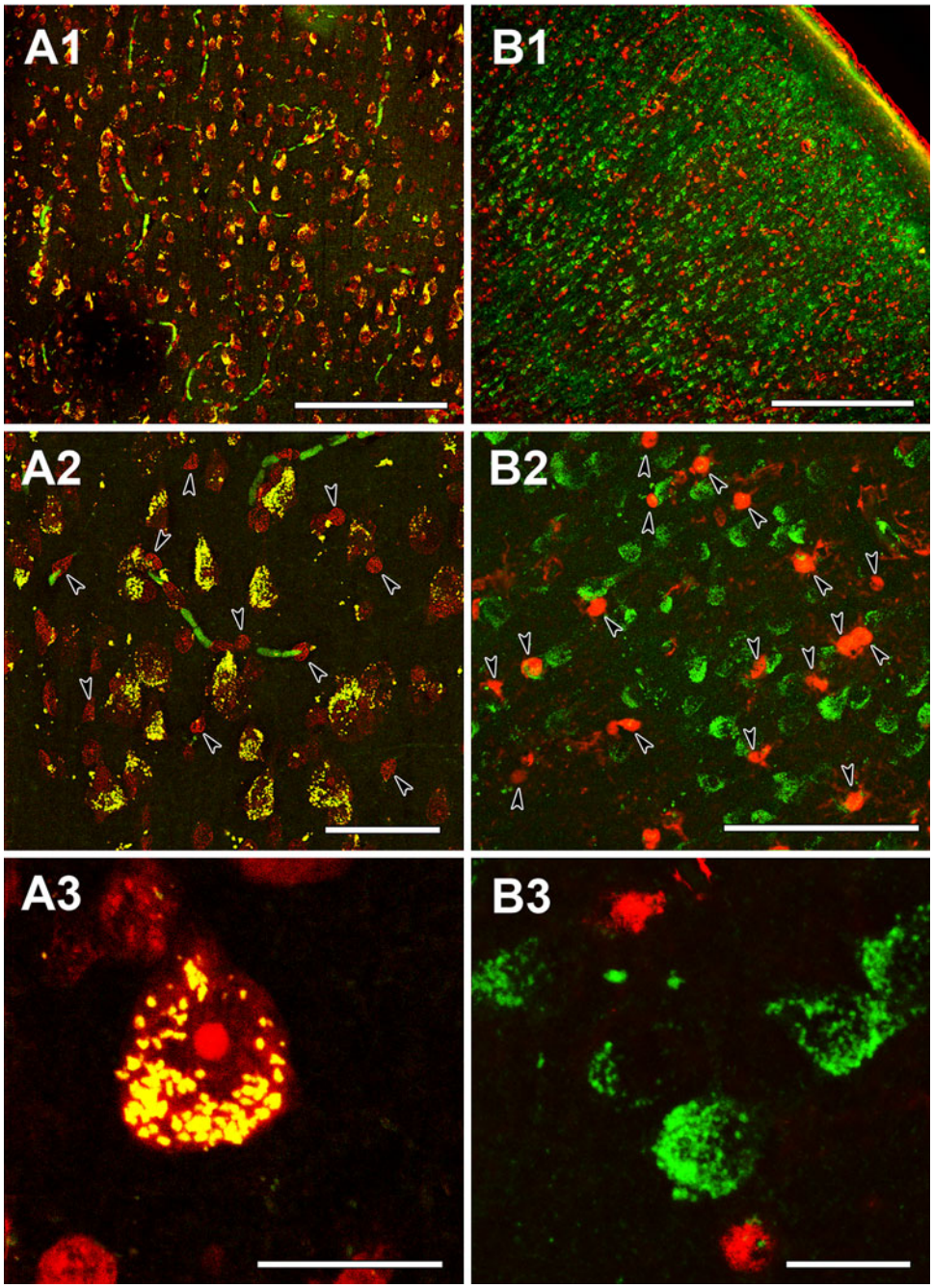

Fig. 4 The neuronal localization of SUCLA2 immunoreactivity in the human temporal cortex. **a1** The distribution of SUCLA2-positive cells is similar to that of Nissl-labeled cells (*red*), both present throughout the temporal cortex. **a2** A higher magnification image reveals that essentially all large Nissl-labeled cells with irregular shape demonstrate SUCLA2 immunolabeling (*yellow cells*). In contrast, small, intensely labeled round-shape cells do not exhibit SUCLA2 immunoreactivity and remain red (*arrowheads*). Some blood vessels are labeled *green* because of the peroxidase activity of the red blood cells present in the vessels in the non-perfused human tissue. **a3** A high-magnification confocal microscopy image demonstrating the punctuate location of SUCLA2 immunoreactivity within the cytosol of Nissl-labeled neurons whereas small glial cells do not exhibit SUCLA2 immunoreactivity. **b1** The distribution of the glial marker S100 (*red*) is different from that of SUCLA2-positive cells (*green*). **b2** A higher magnification image demonstrates lack of co-localization between SUCLA2 and S100. Glial cells labeled with S100 are indicated by arrowheads. **b3** High-magnification confocal picture shows that SUCLA2 and S100 are located in different cell types. *Scale bars* 200 μm for **a1**, 50 μm for **a2**, 20 μm for **a3**, 500 μm for **b1**, 50 μm for **b2**, and 20 μm for **b3**

this, and assuming that diabetes may upregulate SUCLG2 expression in the human brain, we compared SUCLG2 (and SUCLA2) immunoreactivity in brain tissue homogenates from four controls versus four patients that suffered from diabetes mellitus for several years (Table 1c, d) The results are shown in panel C of Fig. 8: SUCLG2 immunoreactivity was not increased in the samples from the diabetic patients as compared to those from control subjects, also verified by densitometric analysis of the bands (not shown). This result affords further credibility to the claim that *SUCLG2* is not expressed in the human brain to a significant extent.

Discussion

Here, we have investigated the cell-specific expression of *SUCLA2* and *SUCLG2* in the human brain. The most important observation was that A-SUCL-β was present

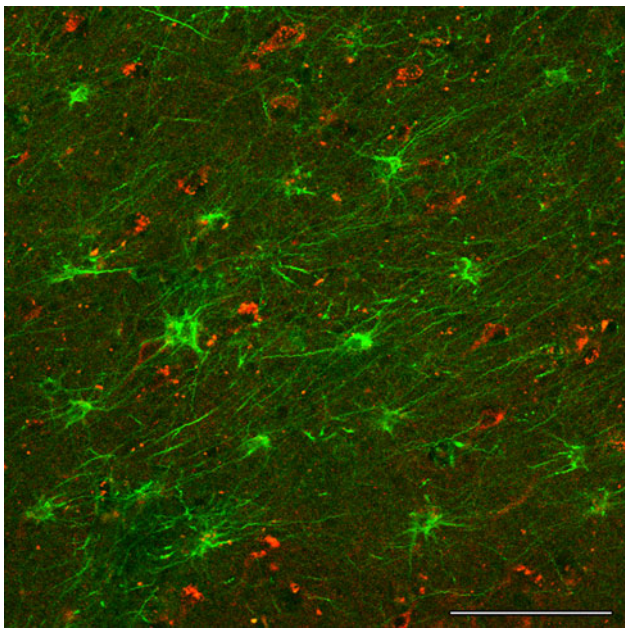

Fig. 5 The different cellular localization of SUCLA2 and GFAP. SUCLA2 labels a number of evenly distributed cells with punctuate appearance (*red*). GFAP-positive glial cells (*green*) possessing the characteristic glial processes are also evenly distributed. These glial cells, however, are not labeled by SUCLA2 whereas SUCLA2 cells are not labeled by GFAP. *Scale bar* 100 μm

exclusively in neurons, and not in other cell types. An obvious pathophysiological implication for astrocytes lacking A-SUCL-β and therefore being incapable of ATP provision by matrix substrate-level phosphorylation, is that their mitochondria are more likely to engage in cytosolic ATP consumption (Chinopoulos et al. 2010) than neuronal mitochondria, during natural fluctuations of their membrane potentials (Gerencser et al. 2012). As an extension of this, astrocytic mitochondria should be more vulnerable than neuronal mitochondria in terms of relying on—in house—ATP reserves during energy crisis, such as during brain ischemia (Chinopoulos and Adam-Vizi 2010; Chinopoulos 2011a, b). To this end, the weak expression of nm23-H4 (Milon et al. 1997), together with the lack of G-SUCL-β expression in astrocytes preclude the possibility of matrix ATP formation through GTP transphosphorylation.

Furthermore, the notion that both ATP- and GTP-forming SUCL activity should exhibit an extremely low—if any—rate in human astrocytes, hints at peculiarities of the directionality of citric acid cycle in these cells (Chinopoulos 2013). Although the citric acid cycle is branded as a "cycle", it does not necessarily operate as one (Chinopoulos 2013). It is well known, that astrocytes produce and release large quantities of succinate (Westergaard et al. 1994). Succinate can be the end-product of a 'backflux' citric acid cycle (Brekke et al. 2012), commencing from pyruvate that is converted to oxaloacetate by pyruvate carboxylase. Pyruvate carboxylase is mostly expressed in liver and kidneys being part of gluconeogenesis, but it is also found in the astrocytes of the brain (Shank et al. 1985; Yu et al. 1983), playing an important role in lipogenesis and synthesis of neurotransmitters (Wallace et al. 1998; Sonnewald and Rae 2010).

Another relevant concept to our findings is that GABA uptake in the neuropil occurs through the GABA transporter GAT-3, which is exclusively expressed in astrocytes (Minelli et al. 1996), as well as GAT-1 and -2, which are found both in astrocytic processes and other neuronal- and non-neuronal elements (Conti et al. 1998, 1999). GABA metabolism in the astrocytes proceeds through GABA transaminase (which also requires α-ketoglutarate) yielding succinate semialdehyde (and glutamate) that is in turn processed by succinate semialdehyde dehydrogenase yielding succinate which enters the citric acid cycle, thus effectively by-passing the 'missing' SUCL, since neither *SUCLA2* nor *SUCLG2* is expressed in these cells.

Finally, in the absence of either ATP- or GTP-forming SUCL, succinyl-CoA emerging from the α-ketoglutarate dehydrogenase complex in astrocytic mitochondria could be further processed towards heme and/or ketone body metabolism, pathways which are fully operational in astrocytes (Lopes-Cardozo et al. 1986; Dringen et al. 2007), or serve as cofactor for lysine succinylation (Zhang et al. 2011), a wide-spread post-translational modification; this would also prevent a 'coenzyme A trap' in the form of succinyl-CoA.

In aggregate, our findings presented in this paper have strong physiological implications regarding the differential metabolism of neurons versus astrocytes in the human brain and pathological implications related to the impact of SUCLA2 deficiency on brain functions. Furthermore, our study pinpoints SUCLA2 as a reliable marker for neuronal mitochondria. By the same token, any report on the function or activity of ATP-forming SUCL in brain tissue should not apply for the whole brain, only for neurons. Finally, and in the same line, intracellular pathological manifestations of the brain caused by SUCLA2 deficiency, such as mtDNA depletion, should only be sought in neurons.

Materials and methods

Human brains

Human brain samples were collected in accordance with the Ethical Rules for Using Human Tissues for Medical Research in Hungary (HM 34/1999) and the Code of Ethics of the World Medical Association (Declaration of

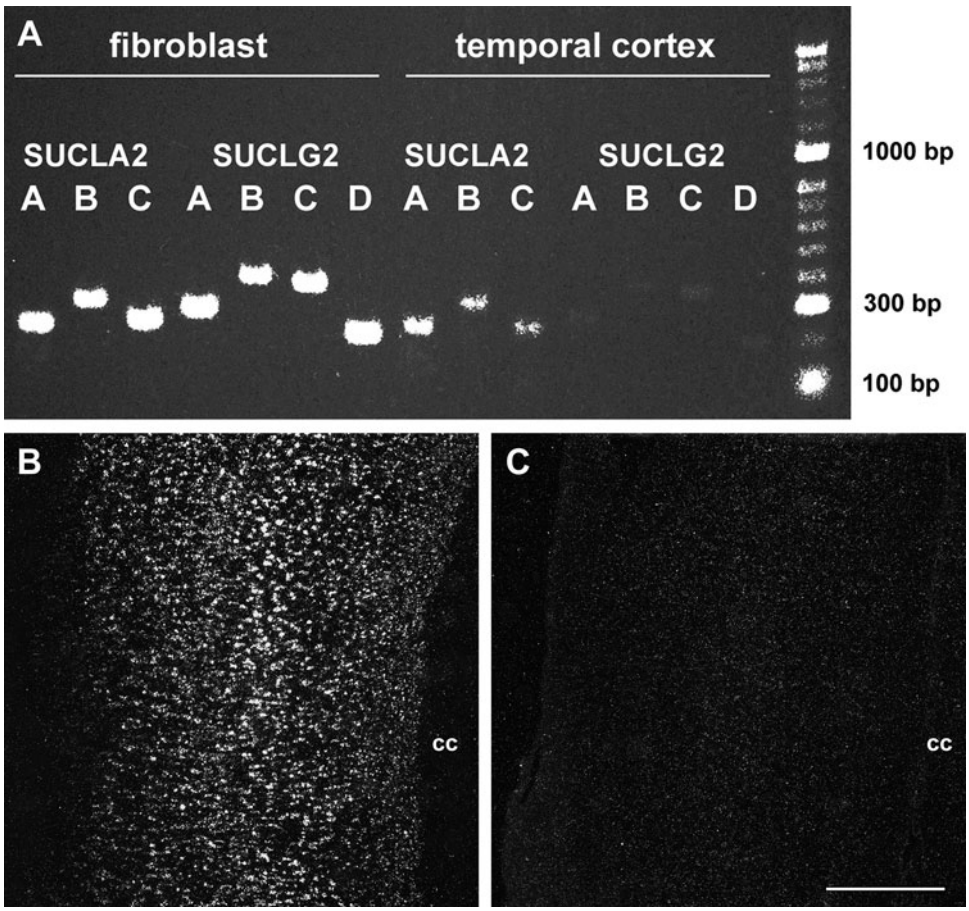

Fig. 6 **a** An RT-PCR experiment demonstrates the expression of SUCLA2 but not SUCLG2 mRNA in the human temporal cortex by showing PCR products run on gel. The appearance of appropriate bands on the gel for primer pairs A–C for *SUCLA2* (235, 309, and 242 bp, respectively) and primer pairs A–D for *SUCLG2* (279, 387, 366, and 211 bp, respectively) in human fibroblasts indicate *SUCLA2* and *SUCLG2* expression in this cell type. In contrast, when the template of the PCR reaction was cDNA prepared from freshly dissected surgical human temporal cortex samples, only *SUCLA2* but not *SUCLG2* resulted in visible bands. Dark-field photomicrographs of human temporal cortex labeled with in situ hybridization histochemistry for *SUCLA2* (**b**), and *SUCLG2* (**c**). The *white dots* represent labeled cells. All cortical layers but not the corpus callosum (cc) is labeled for *SUCLA2* (**b**). The intensity of labeling is highest in layers III–V whereas layers I, II, and VI contains less intensely labeled cells. In contrast, *SUCLG2* labeling above the background is absent in all layers of the cerebral cortex (**c**). *Scale bar* 1 mm

Helsinki). Post mortem tissue samples were taken during brain autopsy. In addition, surgical brain samples were obtained from tissue removed during brain surgeries at the Department of Neurosurgery Medical School, University of Pécs in the framework of the Human Brain Tissue Bank, Budapest. For autopsy, brains were removed from the skull with a post mortem delay of 2–6 h. Prior written informed consent was obtained from the patients or from the next of kin for autopsies, which included the request to conduct neurochemical analyses. The protocols including analyses of tissue samples were approved by institutional ethics committee of the Semmelweis University and the University of Pécs. The three surgical patients underwent the removal of brain tumors. The 11 subjects, whose brains were used in the autopsy study died without any known neurological or affective disorder. The medical history of the subjects was obtained from medical or hospital records, interviews with family members and relatives, as well as from pathological and neuropathological reports. All personal identifiers had been removed and samples were coded before the analyses of tissue.

Surgically dissected freshly frozen temporal cortical samples from a 66-year-old woman were used for RT-PCR and the development of in situ hybridization probes. In situ hybridization histochemistry was performed in temporal cortical samples from this patient as well as in the temporal cortex from a 64-year-old woman. Immunolabeling was performed using frontal cortical sample of a 58-year-old man and temporal cortical samples from the 64-year-old and the 66-year-old woman; tissue blocks of the latter two patients were also used for in situ hybridization histochemistry. Surgical samples that underwent immediate freezing for situ hybridization

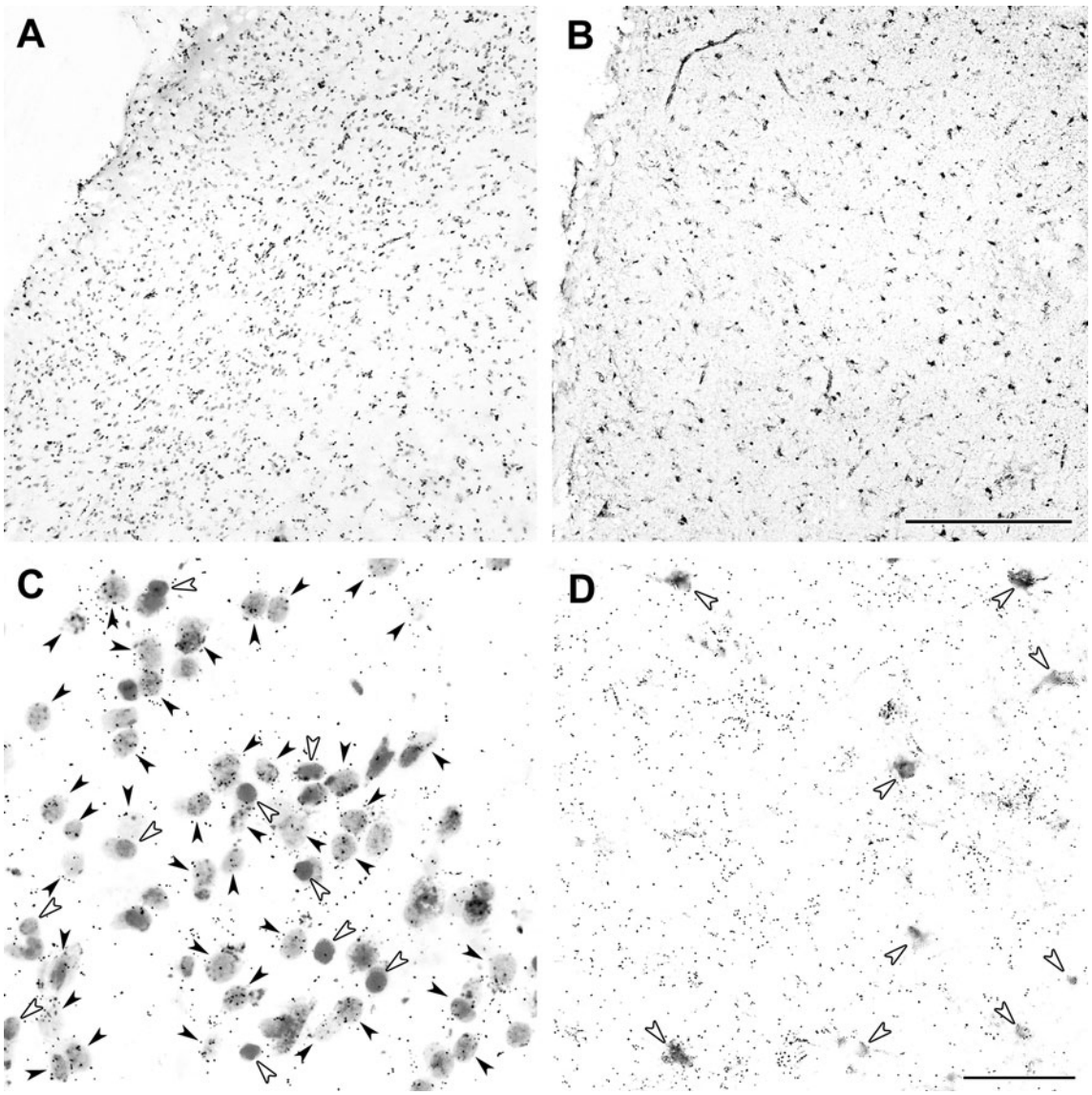

Fig. 7 The selective *SUCLA2* mRNA expression in neurons based on double labeling with in situ hybridization histochemistry for *SUCLA2* and neuronal or glial markers. The distribution of Nissl-labeled cells (**a**) and S100-immunoreactive astrocytes (**b**) is shown in the human temporal cortex. The tiny autoradiography grains of the in situ hybridization signal are not visible at this low magnification. High-magnification pictures demonstrate the location of autoradiography grains representing SUCLA2 mRNA in relation to Nissl-labeled cells (**c**), and S100-immunoreactive astrocytes (**d**). *Black arrowheads* indicate double-labeled cells. Based on the larger size and fainter Nissl labeling, these cells are neurons. Above these cells, the number of autoradiography grains is more than four. In contrast, the darker, smaller and circular-shaped glial cells indicated by *white arrowheads* in **c** are not labeled for *SUCLA2* mRNA. Also, mRNA expression of *SUCLA2* is absent in S100-immunoreactive astrocytes (*white arrowheads*) in **d**. *Scale bars* 500 μm for **a**, **b** and 50 μm for **c**, **d**

histochemistry or immediate fixation for immunolabeling were used in histochemical techniques, because they provided markedly superior results for visualizing *SUCLA2* expression and distribution as compared to post mortem samples.

For western blotting, autopsy samples from different brain regions of 11 subjects were obtained by microdissection. Individual brain nuclei were microdissected from postmortem brains (that have been rapidly frozen on dry ice and stored at −80 °C) using the micropunch technique (Palkovits 1973). Briefly, brains were cut as 1.0−1.5 mm thick coronal sections, and individual brain regions and nuclei were removed by special punch needles with an inside diameter of 1.0–3.5 mm, using either a head magnifier or a stereomicroscope. The microdissected samples were collected in airtight plastic (Eppendorf) tubes and stored at −80 °C until further use. The temperature of brain sections and the microdissected samples was kept under 0 °C during the whole procedure.

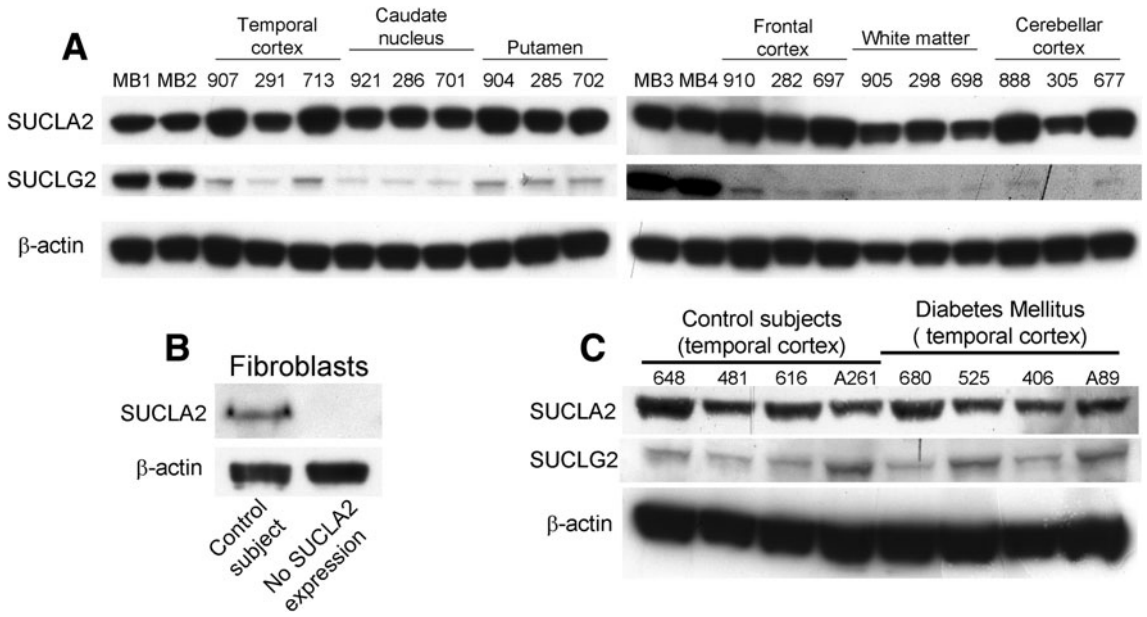

Fig. 8 Immunoreactivities of the substrate-specific β subunit encoded by either SUCLA2 or SUCLG2 in tissue homogenates. **a** MB signifies mouse brain (whole brain homogenates from four different animals 1, 2, 3 and 4). All other alphanumeric titles signify human brain samples obtained from regions as indicated in the panels. **b** Immunoreactivity of the substrate-specific β subunit encoded by SUCLA2 in human fibroblasts from a healthy donor and a patient with a complete deletion of SUCLA2. **c** Immunoreactivities of the substrate-specific β subunit encoded by either SUCLA2 or SUCLG2 in human temporal cortex samples from control subjects versus those that suffered from diabetes mellitus. For all lanes of all panels, immunoreactivity of β-actin was used as a loading control

Mouse brains

Wild type C57BL/6 mice were obtained from Jackson Laboratory (JAX® Mice repository, Bar Harbor, Maine, USA). The animals used in our study were of either sex and 5 and 6 months of age. Mice were housed in a room maintained at 20–22 °C on a 12-h light–dark cycle with food and water available *ad libitum*. All experiments were approved by the Animal Care and Use Committee of the Semmelweis University (Egyetemi Állatkísérleti Bizottság). Mice were killed by cervical dislocation and their brains were removed and kept at −80 °C until further manipulations.

Cell cultures

Fibroblast cultures from skin biopsies from the patient with no SUCLA2 expression and control subjects were prepared. Cells were grown on poly-L-ornithine coated 25 mm round glass coverslips for 5–7 days, at a density of approximately 8×10^5 cells/coverslip in RPMI 1640 medium (GIBCO, Life technologies, Carlsbad, CA, USA) supplemented with 10 % fetal bovine serum and 2 mM glutamine and kept at 37 °C in 5 % CO_2. The medium was also supplemented with penicillin, streptomycin and amphotericin (item A5955, Sigma-Aldrich St. Louis, MO, USA). HEK293 cells were grown on poly-L-ornithine coated 25 mm round glass coverslips for 1–2 days, at a density of approximately 5×10^5 cells/coverslip in DMEM (GIBCO) plus glutamine plus 10 % fetal calf serum and 1 % streptomycin–penicillin.

Tissue collection for immunolabeling

For immunocytochemistry, brains were cut into 5–10 mm thick coronal slices and immersion fixed in 4 % paraformaldehyde in 0.1 M phosphate-buffered saline (PBS) for 3–5 days. Subsequently, the blocks were transferred to PBS containing 0.1 % sodium azide for 2 days to remove excess paraformaldehyde. Then the blocks were placed in PBS containing 20 % sucrose for 2 days for cryoprotection, after which the blocks were frozen and cut into 50 μm thick serial coronal sections on a sliding microtome. Sections were collected in PBS containing 0.1 % sodium azide and stored at 4 °C until further processing.

DAB immunolabeling of brain sections

Every fifth free-floating brain section of human temporal and frontal cortical blocks was immunostained for SUCLA2 and SUCLG2. The antibodies (at dilutions 1:80, 1:320, 1:1,280, 1:5,120) were applied for 48 h at room temperature, followed by incubation of the sections in biotinylated anti-rabbit secondary antibody (1:1,000 dilution, Vector Laboratories, Burlingame, CA) and then in

Table 1 Inventory of human brain samples used for Western blotting in Fig. 8

(a) Brain sample number (control)	Gender	Age	Post mortem delay (h)	Cause of death
910, 905, 907, 921, 904, 888	Male	46	4	Senile, hypertensive atherosclerosis; acute myocardial infarction
282, 298, 291, 286, 285, 305	Male	66	4.5	Cardiovascular-pulmonary insufficiency, acute lymphoid leukemia
697, 698, 713, 701, 702, 677	Male	63	3.5	Pulmonary embolism

(b) Brain region	Sample no.	Sample no.	Sample no.
Frontal cortex	910	282	697
Cerebral white matter (frontal)	905	298	698
Temporal cortex	907	291	713
Caudate nucleus	921	286	701
Putamen	904	285	702
Cerebellar cortex	888	305	677

(c) Brain sample number (control, temporal cortex)	Gender	Age	Post mortem delay (h)	Cause of death
648	Female	72	4	Acute myocardial infarction, earlier heart failure, atherosclerosis
481	Female	89	2	Atherosclerosis cerebri, dementia
616	Female	71	6	Stroke-cardiovascular-pulmonary insufficiency
A261	Female	87	6	Dementia, myocardial insufficiency

(d) Brain sample number (diabetes mellitus, temporal cortex)	Gender	Age	Post mortem delay (h)	Cause of death
680	Female	88	2.5	Cardiac insufficiency, heart failure
525	Female	70	6	Guillain–Barré syndrome
406	Female	68	3	Pneumonia, respiratory insufficiency
A89	Female	79	6	Pulmonary embolism

avidin–biotin-peroxidase complex (1:500, Vector Laboratories) for 2 h. Subsequently, the labeling was visualized by incubation in 0.02 % 3,3-diaminobenzidine (DAB; Sigma), 0.08 % nickel (II) sulfate and 0.001 % hydrogen peroxide in PBS, pH 7.4 for 5 min. Sections were mounted, dehydrated and coverslipped with Cytoseal 60 (Stephens Scientific, Riverdale, NJ, USA).

Double labeling of SUCLA2 in brains sections

SUCLA2 was immunolabeled as for single labeling using 1:1,000 dilution except for the visualization, which was performed with fluorescein isothiocyanate (FITC)-tyramide (1:8,000) and H_2O_2 in 100 mM Trizma buffer (pH 8.0 adjusted with HCl) for 6 min. Subsequently, sections were placed in mouse anti-subunit d of the F_0–F_1 ATP synthase (1:500), or mouse anti-S100, a marker of glial cells (1:500, Millipore, Cat. No. MAB079-1) for 48 h at room temperature. The sections were then incubated in Alexa 594 donkey anti-mouse secondary antibody (1:500, Molecular Probes, Eugene, OR) for 2 h and washed. For the double labeling with Nissl staining, the sections were incubated in 'Neurotrace' red fluorescent Nissl stain (Molecular Probes) diluted to 1:30 for 2 h, and washed in PBS overnight. For double labeling with glial fibrillary acidic protein (GFAP), a marker of glial cells, the sections were first incubated in mouse anti-GFAP (1:300, Santa Cruz Biotechnology, Delaware, CA, USA; Cat. No. sc-33673) and developed with FITC-tyramide amplification immunofluorescence as described above for SUCLA2. Then, the anti-SUCLA2 antiserum was used at a 1:350 dilution and visualized by Alexa 594 donkey anti-rabbit secondary antibody (1:500, Molecular Probes). Finally, all sections with fluorescent labels were mounted on positively charged slides (Superfrost Plus, Fisher Scientific, Pittsburgh, PA) and coverslipped in antifade medium (Prolong Antifade Kit, Molecular Probes).

Immunocytochemistry of cell cultures

Fibroblasts or HEK293 cell cultures were first treated with 1 μM Mitotracker Orange (MTO) for 5 min in their culture media, at 37 °C in 5 % CO_2. Subsequent immunocytochemistry of the cultures was performed by fixing the cells with 4 % paraformaldehyde in PBS for 20 min, followed by permeabilization by 0.1 % TX-100 (in PBS) for 10 min and several washing steps in between with PBS at room temperature. Cultures were treated with 10 % donkey serum overnight at 4 °C followed by bathing in 1 % donkey serum and 1 μg/ml anti-SUCLA2 (Proteintech Europe Ltd, Manchester, UK, Cat. No. #12627-1-AP) or 1 μg/ml anti-SUCLG2 (Abcam, Cambridge, UK, Cat. No. #ab96172) for 1 h at room temperature. Cells were subsequently decorated using the appropriate Cy2- or Alexa 488-linked secondary antibody (1:4,000, donkey anti-rabbit, Jackson Immunochemicals Europe Ltd, Cambridgeshire, UK) in the presence of 1 % donkey serum.

Western blotting

Cultured fibroblasts were harvested by trypsinization. Frozen brain samples were thawn on ice in the presence of radioimmunoprecipitation assay buffer and a protease cocktail inhibitor containing: 0.5 mM 4-(2-aminoethyl) benzenesulfonyl fluoride hydrochloride, 150 nM Aprotinin, 1 μM E-64, 0.5 mM EDTA disodium, and 1 μM Leupeptin, and homogenized with a Teflon pestle. The suspensions were centrifuged once at 10,000*g* for 10 min, and the proteins present in the supernatants were separated by sodium dodecyl sulfate-polyacrylamide gel electrophoresis (SDS-PAGE). Separated proteins were transferred to a methanol-activated polyvinylidene difluoride membrane. Immunoblotting was performed as recommended by the manufacturers of the antibodies. Rabbit polyclonals anti-SUCLG2 (Abcam, Cambridge, UK), and anti-SUCLA2 primary antibodies were used at concentrations of 1 μg/ml, and rabbit polyclonal anti-β actin (Abcam) at 0.1 μg/ml. Immunoreactivity was detected using the appropriate peroxidase-linked secondary antibody (1:4,000, donkey anti-rabbit, Jackson Immunochemicals Europe Ltd, Cambridgeshire, UK) and enhanced chemiluminescence detection reagent (ECL system; Amersham Biosciences GE Healthcare Europe GmbH, Vienna, Austria).

RT-PCR

RNA was isolated from surgically dissected human temporal cortex and cultured human fibroblasts. The surgical brain tissue sample was quickly frozen on dry ice and kept at −80 °C until RNA isolation. The fibroblasts were centrifuged and resuspended in PBS immediately before RNA isolation. Both the brain surgical samples and the fibroblasts were homogenized in Trizol^R Reagent (Invitrogen, Carlsbad, CA, USA) and RNA was isolated according to the manufacturer's instructions. After diluting RNA to 1 μg/μl, it was treated with Amplification Grade DNase I (Invitrogen) and cDNA was synthesized with a SuperScript II reverse transcriptase kit (Invitrogen) according to the manufacturer's instructions. After tenfold dilution, 2.5 μl of the resulting cDNA was used as template in PCR reactions performed with iTaq DNA polymerase (Bio-Rad Laboratories, Hercules, CA, USA) in total volumes of 12.5 μl under the following conditions: 95 °C for 3 min, followed by 35 cycles of 95 °C for 0.5 min, 60 °C for 0.5 min and 72 °C for 1 min. Primers were used at 300 nM final concentration for *SUCLA2* (primer pair A:

CCAGCCAACTTCCTTGATGT and TCAGTGCCTTAG CATCATCG, primer pair B: TGCTGAGTCTCCTGAAG CAA and TCATCTTCCTGGGTCCAGTC, primer pair C: GCAGCAGAAAACATGGTCAA and CCATCGAGGCC AATGTAGTT), and *SUCLG2* (primer pair A: GAAGCTC TCGAGGCTGCTAA and GTCCATCAGAATTGCCAG GT, primer pair B: CCCTTTGGTGAAACTCCAGA and AATGATGGCACAGTTGACGA, primer pair C: GGTCC CAGGCAGTTCAATTA and TATCCAAGGCTTCAGCA ACC, primer pair D: CATTGCCTGCTTTGTGAATG and AATGATGGCACAGTTGACGA). The calculated lengths of the PCR products are 235, 309, and 242 base pairs (bp) for human *SUCLA2* (1,081–1,315, 645–953, and 763–1,004 bp of GenBank accession number NM_003850.2), and 279, 387, 366, and 211 bp for human *SUCLG2* (227–505, 758–1,144, 105–470, and 934–1,144 bp of GenBank accession number NM_001177599.1). The primers were chosen to generate probes that recognize all known RNA species for the particular gene. The resulting PCR products are intron-spanning, to detect potential genomic DNA contamination by its larger size. PCR products were run on gel and pictures were taken by a digital camera. Images were cropped and contrast was adjusted using the "levels" command in Adobe Photoshop CS 8.0.

Preparation of in situ hybridization probes

The PCR products using primer pairs A and B for both *SUCLA2* and *SUCLG2* were purified from gel to obtain non-overlapping probes to demonstrate specific labeling. The purified PCR products were inserted into TOPO TA cloning vectors (Invitrogen) and transformed chemically into competent bacteria according to the manufacturer's instructions. Plasmids were purified from 5 to 7 colonies and applied as templates in PCR reactions with the specific primer pairs to select plasmids containing specific inserts. A positive plasmid for each probe was applied as template in PCR reactions, using primer pairs specific for the probe and also containing T7 RNA polymerase recognition site (GTAATACGACTCACTATAGGGCGAATTGGGTA) added to the reverse primers. Finally, the identities of the cDNA probes were verified by sequencing them with T7 primers.

In situ hybridization histochemistry

Surgically dissected temporal cortical brain samples from two patients were quickly frozen on dry ice, and kept at −80 °C. Serial coronal sections (12 μm thick) were cut using a cryostat, mounted on positively charged slides (Superfrost Plus), dried, and stored at −80 °C until use. [^{35}S] UTP-labeled riboprobes were generated from the DNA probes containing T7 RNA polymerase recognition sites using a MAXIscript transcription kit (Ambion, Austin, TX, USA). The preparation of tissue was performed using mRNA locator Kit (Ambion), according to the manufacturer's instructions. For hybridization, we used 80 μl hybridization buffer (mRNA locator Kit; Ambion) and labeled probes of 1 million DPM activity per slide. Washing procedures included a 30 min incubation in RNase A followed by decreasing concentrations of sodium-citrate buffer (pH 7.4) at room temperature and subsequently at 65 °C. Following successive dehydration and drying, the slides were dipped in 'NTB' nuclear track emulsion (Eastman Kodak, Rochester, NY, USA) and stored at 4 °C for 3 weeks. Then the slides were developed and fixed with Kodak Dektol developer and Kodak fixer, respectively, counterstained with Giemsa, and coverslipped with Cytoseal 60 (Stephens Scientific). A cell was considered to express *SUCLA2* or *SUCLG2* if the number of autoradiography grains accumulated in a seemingly Gaussian distribution around a center was at least three times higher than the background level in an area corresponding to an average cell size (a circle with a diameter of 25 μm) in the same section. The background typically consisted of 1–3 grains per cell.

Combination of in situ hybridization histochemistry with Nissl staining

Slide attached sections of fresh temporal cortical brain tissue were first processed for in situ hybridization, as described above. After development, the sections were stained with 0.1 % cresyl-violet dissolved in PBS, and then immersed in 96 % ethanol containing 0.01 % acetic acid. Alternatively, the sections were incubated in 'Neurotrace' red fluorescent Nissl stain (Molecular Probes,) diluted to 1:30 for 2 h, washed in PBS overnight, and coverslipped in antifade medium (Prolong Antifade Kit, Molecular Probes). A cell was considered glial if it was dark labeled, and had a small diameter round-shape appearance. In turn, neurons exhibited less intense labeling, were larger and their shape was less regularly rounded. A cell was considered *SUCLA2*-expressing if it met the criteria described above for single label in situ hybridization histochemistry. A *SUCLA2*-expressing cell was considered Nissl-labeled if at least 70 % of the area of the circle containing the accumulation of autoradiography grains contained Nissl labeling, and the center of the autoradiography grains was within the Nissl labeling.

Combination of in situ hybridization histochemistry with S100 immunohistochemistry

Slide attached sections (20 μm thick) of fixed temporal cortical brain brains were first processed for in situ

hybridization, as described above. Thus, tightly bound RNA–RNA pairs were already formed by the time immunohistochemistry was performed, immediately before dipping the slides into autoradiographic emulsion. In addition, the solutions used for perfusion and immunohistochemistry were prepared with DAPC-treated RNAse-free water, which ensured that the labeling intensity of the in situ hybridization histochemistry did not decrease significantly. The immunolabeling protocol for S100 was the same as that described above for double labeling immunohistochemistry. Immunoreactivity was visualized using DAB reactions, after which the in situ hybridization procedure was continued by dipping the slides into the emulsion. Each double labeling experiment included controls, which was carried out through the double labeling procedure without application of radioactive in situ hybridization probes. These controls demonstrated that the DAB signal did not induce an autoradiography signal. A *SUCLA2*-expressing cell was considered S100-immunopositive if at least 70 % of the area of the circle containing the accumulation of autoradiography grains contained immunoreactivity for S100 and the center of the autoradiography grains was within the immunolabeled cell.

Image processing

The sections were examined using an Olympus BX60 light microscope equipped with bright-field, dark-field and fluorescence. Images were captured at 2,048 × 2,048 pixel resolution with a SPOT Xplorer digital CCD camera (Diagnostic Instruments, Sterling Heights, MI, USA) using a 4× objective for dark-field images, and 4–40× objectives for bright-field and fluorescent images. *Fluorescent sections* were also evaluated using a Bio-Rad 2100 Rainbow Confocal System (Bio-Rad Laboratories, Inc, CA, USA). The contrast and sharpness of the images were adjusted using the "levels" and "sharpness" commands in Adobe Photoshop CS 8.0. Full resolution was maintained until the photomicrographs were finally cropped at which point the images were adjusted to a resolution of 300 dpi.

Analysis of double immunolabeling

Three 1 × 1 mm areas of double-labeled remote sections from each brain were randomly selected. The total number of SUCLA2-positive neurons with an identifiable cell nucleus and the number of double-labeled cells was counted using a 20× objective of an Olympus BX60 light microscope equipped with fluorescent epi-illumination and a filter allowing for visualization of both green and red colors. Subsequently, the number of single labeled cells was also calculated in the area.

Acknowledgments Thanks are expressed to Katalin Zölde for excellent technical assistance.This work was supported by the Országos Tudományos Kutatási Alapprogram (OTKA) grants NNF2 85612, K 100319 to A.D., the Danish National Health Research Council grant 12-127702 to E.O., OTKA 81983 and the Hungarian Academy of Sciences grant 02001 to V. A.-V, TÁMOP 4.2.1./B-09/1/KMR and BIOINF09TÉT_10-1-2011-0058 to MJM, OTKA grants NNF 78905, NNF2 85658, K 100918, and the MTA-SE Lendület Neurobiochemistry Research Division grant 95003 to C.C.

Conflict of interest The authors declare no conflict of interests.

References

Brekke E, Walls AB, Norfeldt L, Schousboe A, Waagepetersen HS, Sonnewald U (2012) Direct measurement of backflux between oxaloacetate and fumarate following pyruvate carboxylation. Glia 60:147–158

Carrozzo R, Dionisi-Vici C, Steuerwald U, Lucioli S, Deodato F, Di Giandomenico S, Bertini E, Franke B, Kluijtmans LAJ, Meschini MC, Rizzo C, Piemonte F, Rodenburg R, Santer R, Santorelli FM, van Rooij A, Vermunt-de Koning D, Morava E, Wevers RA (2007) SUCLA2 mutations are associated with mild methylmalonic aciduria, leigh-like encephalomyopathy, dystonia and deafness. Brain 130:862–874

Chinopoulos C (2011a) Mitochondrial consumption of cytosolic ATP: not so fast. FEBS Lett 585:1255–1259

Chinopoulos C (2011b) The "B Space" of mitochondrial phosphorylation. J Neurosci Res 89:1897–1904

Chinopoulos C (2013) Which way does the citric acid cycle turn during hypoxia? The critical role of alpha-ketoglutarate dehydrogenase complex. J Neurosci Res 91:1030–1043

Chinopoulos C, Adam-Vizi V (2010) Mitochondria as ATP consumers in cellular pathology. Biochim Biophys Acta 1802:221–227

Chinopoulos C, Gerencser AA, Mandi M, Mathe K, Torocsik B, Doczi J, Turiak L, Kiss G, Konrad C, Vajda S, Vereczki V, Oh RJ, Adam-Vizi V (2010) Forward operation of adenine nucleotide translocase during F0F1-ATPase reversal: critical role of matrix substrate-level phosphorylation. FASEB J 24:2405–2416

Conti F, Melone M, De BS, Minelli A, Brecha NC, Ducati A (1998) Neuronal and glial localization of GAT-1, a high-affinity gamma-aminobutyric acid plasma membrane transporter, in human cerebral cortex: with a note on its distribution in monkey cortex. J Comp Neurol 396:51–63

Conti F, Zuccarello LV, Barbaresi P, Minelli A, Brecha NC, Melone M (1999) Neuronal, glial, and epithelial localization of gamma-aminobutyric acid transporter 2, a high-affinity gamma-aminobutyric acid plasma membrane transporter, in the cerebral cortex and neighboring structures. J Comp Neurol 409:482–494

Dringen R, Bishop GM, Koeppe M, Dang TN, Robinson SR (2007) The pivotal role of astrocytes in the metabolism of iron in the brain. Neurochem Res 32:1884–1890

Elpeleg O, Miller C, Hershkovitz E, Bitner-Glindzicz M, Bondi-Rubinstein G, Rahman S, Pagnamenta A, Eshhar S, Saada A (2005) Deficiency of the ADP-forming succinyl-CoA synthase activity is associated with encephalomyopathy and mitochondrial DNA depletion. Am J Hum Genet 76:1081–1086

Gerencser AA, Chinopoulos C, Birket MJ, Jastroch M, Vitelli C, Nicholls DG, Brand MD (2012) Quantitative measurement of mitochondrial membrane potential in cultured cells: calcium-induced de- and hyperpolarization of neuronal mitochondria. J Physiol 590:2845–2871

Jenkins TM, Weitzman PD (1986) Distinct physiological roles of animal succinate thiokinases. Association of guanine nucleotide-linked succinate thiokinase with ketone body utilization. FEBS Lett 205:215–218

Johnson JD, Mehus JG, Tews K, Milavetz BI, Lambeth DO (1998) Genetic evidence for the expression of ATP- and GTP-specific succinyl-CoA synthetases in multicellular eucaryotes. J Biol Chem 273:27580–27586

Kadrmas EF, Ray PD, Lambeth DO (1991) Apparent ATP-linked succinate thiokinase activity and its relation to nucleoside diphosphate kinase in mitochondrial matrix preparations from rabbit. Biochim Biophys Acta 1074:339–346

Kiss G, Konrad C, Doczi J, Starkov AA, Kawamata H, Manfredi G, Zhang SF, Gibson GE, Beal MF, Adam-Vizi V, Chinopoulos C (2013) The negative impact of alpha-ketoglutarate dehydrogenase complex deficiency on matrix substrate-level phosphorylation. FASEB J 27:2392–2406

Kowluru A, Tannous M, Chen HQ (2002) Localization and characterization of the mitochondrial isoform of the nucleoside diphosphate kinase in the pancreatic beta cell: evidence for its complexation with mitochondrial succinyl-CoA synthetase. Arch Biochem Biophys 398:160–169

Labbe RF, Kurumada T, Onisawa J (1965) The role of succinyl-CoA synthetase in the control of heme biosynthesis. Biochim Biophys Acta 111:403–415

Lambeth DO, Tews KN, Adkins S, Frohlich D, Milavetz BI (2004) Expression of two succinyl-CoA synthetases with different nucleotide specificities in mammalian tissues. J Biol Chem 279:36621–36624

Li X, Wu F, Beard DA (2013) Identification of the kinetic mechanism of succinyl-CoA synthetase. Biosci Rep 33:145–163

Lopes-Cardozo M, Larsson OM, Schousboe A (1986) Acetoacetate and glucose as lipid precursors and energy substrates in primary cultures of astrocytes and neurons from mouse cerebral cortex. J Neurochem 46:773–778

McKee EE, Bentley AT, Smith RM Jr, Ciaccio CE (1999) Origin of guanine nucleotides in isolated heart mitochondria. Biochem Biophys Res Commun 257:466–472

McKee EE, Bentley AT, Smith RM Jr, Kraas JR, Ciaccio CE (2000) Guanine nucleotide transport by atractyloside-sensitive and -insensitive carriers in isolated heart mitochondria. Am J Physiol Cell Physiol 279:C1870–C1879

Miller C, Wang L, Ostergaard E, Dan P, Saada A (2011) The interplay between SUCLA2, SUCLG2, and mitochondrial DNA depletion. Biochim Biophys Acta 1812:625–629

Milon L, Rousseau-Merck MF, Munier A, Erent M, Lascu I, Capeau J, Lacombe ML (1997) nm23-H4, a new member of the family of human nm23/nucleoside diphosphate kinase genes localised on chromosome 16p13. Hum Genet 99:550–557

Minelli A, DeBiasi S, Brecha NC, Zuccarello LV, Conti F (1996) GAT-3, a high-affinity GABA plasma membrane transporter, is localized to astrocytic processes, and it is not confined to the vicinity of GABAergic synapses in the cerebral cortex. J Neurosci 16:6255–6264

Navarro-Sastre A, Tort F, Garcia-Villoria J, Pons MR, Nascimento A, Colomer J, Campistol J, Yoldi ME, Lopez-Gallardo E, Montoya J, Unceta M, Martinez MJ, Briones P, Ribes A (2012) Mitochondrial DNA depletion syndrome: new descriptions and the use of citrate synthase as a helpful tool to better characterise the patients. Mol Genet Metab 107:409–415

Ostergaard E (2008) Disorders caused by deficiency of succinate-CoA ligase. J Inherit Metab Dis 31:226–229

Ostergaard E, Christensen E, Kristensen E, Mogensen B, Duno M, Shoubridge EA, Wibrand F (2007a) Deficiency of the alpha subunit of succinate-coenzyme A ligase causes fatal infantile lactic acidosis with mitochondrial DNA depletion. Am J Hum Genet 81:383–387

Ostergaard E, Hansen FJ, Sorensen N, Duno M, Vissing J, Larsen PL, Faeroe O, Thorgrimsson S, Wibrand F, Christensen E, Schwartz M (2007b) Mitochondrial encephalomyopathy with elevated methylmalonic acid is caused by SUCLA2 mutations. Brain 130:853–861

Ostergaard E, Schwartz M, Batbayli M, Christensen E, Hjalmarson O, Kollberg G, Holme E (2010) A novel missense mutation in SUCLG1 associated with mitochondrial DNA depletion, encephalomyopathic form, with methylmalonic aciduria. Eur J Pediatr 169:201–205

Ottaway JH, McClellan JA, Saunderson CL (1981) Succinic thiokinase and metabolic control. Int J Biochem 13:401–410

Palkovits M (1973) Isolated removal of hypothalamic or other brain nuclei of the rat. Brain Res 59:449–450

Pall ML (1985) GTP: a central regulator of cellular anabolism. Curr Top Cell Regul 25:1–20

Pfaff E, Klingenberg M, Heldt HW (1965) Unspecific permeation and specific exchange of adenine nucleotides in liver mitochondria. Biochim Biophys Acta 104:312–315

Przybyla-Zawislak B, Dennis RA, Zakharkin SO, McCammon MT (1998) Genes of succinyl-CoA ligase from *Saccharomyces cerevisiae*. Eur J Biochem 258:736–743

Rotig A, Poulton J (2009) Genetic causes of mitochondrial DNA depletion in humans. Biochim Biophys Acta 1792:1103–1108

Shank RP, Bennett GS, Freytag SO, Campbell GL (1985) Pyruvate carboxylase: an astrocyte-specific enzyme implicated in the replenishment of amino acid neurotransmitter pools. Brain Res 329:364–367

Sonnewald U, Rae C (2010) Pyruvate carboxylation in different model systems studied by (13)C MRS. Neurochem Res 35:1916–1921

Strausberg RL, Feingold EA, Grouse LH, Derge JG, Klausner RD, Collins FS, Wagner L, Shenmen CM, Schuler GD, Altschul SF, Zeeberg B, Buetow KH, Schaefer CF, Bhat NK, Hopkins RF, Jordan H, Moore T, Max SI, Wang J, Hsieh F, Diatchenko L, Marusina K, Farmer AA, Rubin GM, Hong L, Stapleton M, Soares MB, Bonaldo MF, Casavant TL, Scheetz TE, Brownstein MJ, Usdin TB, Toshiyuki S, Carninci P, Prange C, Raha SS, Loquellano NA, Peters GJ, Abramson RD, Mullahy SJ, Bosak SA, McEwan PJ, McKernan KJ, Malek JA, Gunaratne PH, Richards S, Worley KC, Hale S, Garcia AM, Gay LJ, Hulyk SW, Villalon DK, Muzny DM, Sodergren EJ, Lu X, Gibbs RA, Fahey J, Helton E, Ketteman M, Madan A, Rodrigues S, Sanchez A, Whiting M, Madan A, Young AC, Shevchenko Y, Bouffard GG, Blakesley RW, Touchman JW, Green ED, Dickson MC, Rodriguez AC, Grimwood J, Schmutz J, Myers RM, Butterfield YS, Krzywinski MI, Skalska U, Smailus DE, Schnerch A, Schein JE, Jones SJ, Marra MA (2002) Generation and initial analysis of more than 15,000 full-length human and mouse cDNA sequences. Proc Natl Acad Sci USA 99:16899–16903

Tanner S, Shen Z, Ng J, Florea L, Guigo R, Briggs SP, Bafna V (2007) Improving gene annotation using peptide mass spectrometry. Genome Res 17:231–239

Thomson M (1998) What are guanosine triphosphate-binding proteins doing in mitochondria? Biochim Biophys Acta 1403:211–218

Vozza A, Blanco E, Palmieri L, Palmieri F (2004) Identification of the mitochondrial GTP/GDP transporter in *Saccharomyces cerevisiae*. J Biol Chem 279:20850–20857

Wallace JC, Jitrapakdee S, Chapman-Smith A (1998) Pyruvate carboxylase. Int J Biochem Cell Biol 30:1–5

Westergaard N, Sonnewald U, Schousboe A (1994) Release of alpha-ketoglutarate, malate and succinate from cultured astrocytes: possible role in amino acid neurotransmitter homeostasis. Neurosci Lett 176:105–109

Yu AC, Drejer J, Hertz L, Schousboe A (1983) Pyruvate carboxylase activity in primary cultures of astrocytes and neurons. J Neurochem 41:1484–1487

Zhang Z, Tan M, Xie Z, Dai L, Chen Y, Zhao Y (2011) Identification of lysine succinylation as a new post-translational modification. Nat Chem Biol 7:58–63